Vortex quasi-crystals in mesoscopic superconducting samples*

Jing-Kun Wang(王璟琨)[1], Wei Zhang(张威)[1,2,†], and Sá de Melo C A R[3]

[1] *Department of Physics, Renmin University of China, Beijing* 100872, *China*

[2] *Beijing Key Laboratory of Opto-electronic Functional Materials and Micro-nano Devices, Renmin University of China, Beijing* 100872, *China*

[3] *School of Physics, Georgia Institute of Technology, Atlanta, Georgia 30332, USA*

(Received 26 February 2016; revised manuscript received 23 April 2016; published online 25 June 2016)

There seems to be a one to one correspondence between the phases of atomic and molecular matter (AMOM) and vortex matter (VM) in superfluids and superconductors. Crystals, liquids, and glasses have been experimentally observed in both AMOM and VM. Here, we propose a vortex quasi-crystal state which can be stabilized due to boundary and surface energy effects for samples of special shapes and sizes. For finite sized pentagonal samples, it is proposed that a phase transition between a vortex crystal and a vortex quasi-crystal occurs as a function of magnetic field and temperature as the sample size is reduced.

Keywords: vortex matter, quasi-crystal, mesoscopic superconductor

PACS: 74.25.Uv, 74.25.Op, 74.78.Na **DOI:** 10.1088/1674-1056/25/8/087401

1. Introduction

The general subject of vortex physics in superconductors is quite interesting since there seems to be a large variety of possible equilibrium vortex phases in superconductors.[1] The term "vortex matter" has been coined to emphasize the complexity and diversity of vortex phases in superconductors when compared to atomic and molecular matter. One can think of a one to one correspondence between phases in atomic and molecular matter (AMOM) and phases in vortex matter (VM). A liquid in AMOM corresponds to a vortex liquid in VM;[2,3] a crystalline lattice in AMOM corresponds to a vortex lattice in VM;[4] an amorphous or glassy solid in AMOM corresponds to an amorphous or glassy vortex system in VM.[5] In addition, a quasi-crystal is another very interesting state which has been experimentally discovered in AMOM,[6] but there are no corresponding experiments for vortex matter.

The possibility of vortex quasi-crystal was initially discussed several years ago,[7] and more recently quasi-periodic arrangements of vortices were discussed in the presence of underlying quasi-periodic pinning potentials.[8–12] In these recent theoretical and experimental studies it was suggested that the physical properties are quite unconventional due to quasi-periodic pinning potentials. However, unlike these studies, the present manuscript is dedicated to a discussion of vortex quasi-crystalline phases in superconductors without quasi-periodic pinning potentials. Our work is also quite distinct from the case encountered in some atomic and molecular matter, where certain types of interactions can lead to colloidal quasi-crystals.[13]

The central question of this manuscript is: under what conditions is a quasi-crystalline arrangement of vortices at all possible? A definite possibility is to argue that a stable vortex quasi-crystal can arise from an imposed quasi-periodic potential like for instance in the case of a superconductor with quasi-periodic pinning potentials,[8,9] or in heterostructures consisting of a superconductor film grown on top of a quasi-crystal film. Another possibility is to create a quasi-periodic optical lattice with laser beams, trap and cool atoms, and produce vortex quasi-crystals in Bose or Fermi superfluids. This experiment is natural since the production of vortex lattices in superfluid Bose or Fermi ultra-cold atoms has become standard,[14,15] and more recently square optical lattices were used to induce transitions between triangular and square vortex lattices using a mask technique.[16] Thus, the generation of 5-fold quasi-periodic optical lattices using a mask with five holes as the vertices of a regular pentagon (or other methods) may also be used to produce transitions between triangular and 5-fold symmetric vortex lattices.

However, in this manuscript, we concentrate on the possibility of stabilizing vortex quasi-crystals only due to boundary effects in finite superconducting samples, where the sample size and shape play an important role. This option is motivated by recent experimental studies of the vortex structure in disk, triangular, square, and star-shaped mesoscopic samples.[17–22] These works provide us with the technique that allows the preparation of pentagonal (pentagon-cylinders) or decagonal (decagonal-cylinders) samples as potential candidates for 5-fold or 10-fold vortex quasi-crystals. Furthermore, in these

*Project supported by the National Natural Science Foundation of China (Grant Nos. 11274009, 11434011, and 111522436), the National Key Basic Research Program of China (Grant No. 2013CB922000), the Research Funds of Renmin University of China (Grant Nos. 10XNL016 and 16XNLQ03), and the Program of State Key Laboratory of Quantum Optics and Quantum Optics Devices (Grant No. KF201404).

†Corresponding author. E-mail: wzhangl@ruc.edu.cn

© 2016 Chinese Physical Society and IOP Publishing Ltd

mesoscopic systems of cross-sectional area A, the number of vortices M is essentially given by $M = HA/\Phi_0$, where Φ_0 is the quantum of flux, and H is the magnetic field. Therefore, samples with large upper critical field H_{c_2} may produce a sufficiently large number of vortices even when the cross-sectional area is small, and the appearance of quasi-crystalline order is a definite possibility. For example, for a sample of cross-sectional area $A = 1\ \mu m^2$ and upper critical field at zero temperature $H_{c_2}(0) = 10$ T, the number of vortices $M \approx 5000$ is quite substantial close to $H_{c_2}(0)$. In addition, since superconductors with large H_{c_2} are usually associated with short coherence lengths, the vortex quasi-crystalline phase proposed here is more likely to be observable in proper samples of short coherence length superconductors at high magnetic fields and low temperatures.

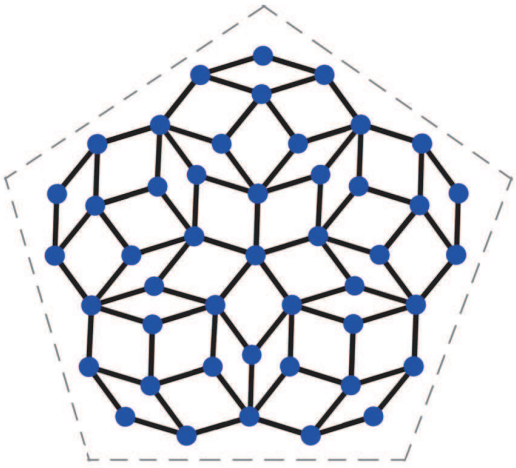


Fig. 1. (color online) We consider a vortex lattice in a pentagon superconducting sample having Penrose tiling with 5-fold rotational symmetry. The tiles consist of two types of lozenges, one with internal angles 36° and 144° (thin lozenge) and the other with internal angles 72° and 108° (thick lozenge), and the vortices (solid circles) are located at the vertices of each lozenge.

This possibility is considered here under the following program. In this manuscript only the case of an isotropic type II superconductor in a magnetic field is considered. First, the bulk free energy is calculated for a triangular, a square and a 5-fold quasi-crystal array. The 5-fold quasi-crystal array is modeled by a Penrose tiling of the plane as shown in Fig. 1. It is shown that the Penrose tile array (vortex quasi-crystal) has a bulk free energy which is just a few percent higher than the triangular array. Second, instead of considering an infinite (bulk) system, a pentagon cylinder sample is discussed. The pentagon cylinder has a pentagonal cross-section (in the x–y plane) with side dimension ℓ, and with height L along the z direction. Here, $L \ll \ell$, such that the pentagon cylinder is essentially two-dimensional and demagnetization effects are small for magnetic fields along the z direction. In this case, when the sample size gets smaller the contribution of the boundaries (surface energy) to the total free energy of the system becomes more important. The surface energy is highly sensitive to the symmetry and to the surface area of the boundaries. Taking into account the surface free energies, it is shown that the Penrose tiling (vortex quasi-crystal) has lower free energy than the triangular lattice in certain regions of the magnetic field versus temperature phase diagram. This is suggestive that a "first order phase transition" may occur between the triangular lattice and the Penrose tiling (vortex quasi-crystal).[1)]

The remainder of this manuscript is organized as follows. In Section 2, we discuss a Ginzburg–Landau approach to obtain the free energy of the triangular, square and Penrose-tiling in the bulk. In Section 3, we present the effects of pentagonal boundaries on the free energy of the triangular lattice and Penrose-tiling, and obtain the critical magnetic field where the transition from a triangular vortex lattice to a vortex quasi-crystal occurs. In Section 4, we discuss thermodynamic quantities including the change in magnetization and entropy, while in Section 5, we discuss neutron scattering, Bitter decoration and scanning tunneling microscopy as possible probes to identify the quasi-crystalline structure. Lastly, in Section 6, we state our conclusions and summarize.

2. Ginzburg–Landau theory

The starting point of our analysis to describe the vortex-quasi-crystal state is the Ginzburg-Landau (GL) free energy density

$$\Delta F_{\rm s} = F_{\rm l} + \frac{1}{2m}\left|\left(-{\rm i}\hbar\nabla - \frac{2e\boldsymbol{A}}{c}\right)\Psi(\boldsymbol{r})\right|^2 + \frac{H^2}{8\pi} \qquad (1)$$

for isotropic superconductors with no disorder, where $\Delta F_{\rm s} = F_{\rm s} - F_{\rm n}$ is the free energy density difference between the superconducting state ($F_{\rm s}$) and the normal state ($F_{\rm n}$), and $F_{\rm l} = \alpha|\Psi(\boldsymbol{r})|^2 + \beta|\Psi(\boldsymbol{r})|^4/2$. It is useful to introduce the dimensionless quantities $f = \Psi\sqrt{-\beta/\alpha}$, $\boldsymbol{\rho} = \boldsymbol{r}/\lambda(T)$, $\mathscr{A} = 2\pi\xi(T)\boldsymbol{A}/\Phi_0$, and $\mathscr{H} = 2\pi\xi(T)\lambda(T)H/\Phi_0$, where λ is the penetration depth, ξ is the coherence length, and $\Phi_0 = hc/2e$ is the flux quantum. Here, $f = f_0\exp({\rm i}\phi)$, and $\mathscr{A} = \mathscr{A}_0 + \nabla\phi/\kappa$ with $\kappa = \lambda/\xi$ the GL parameter. Notice that when $f_0 = 1$ the system is fully superconducting, and when $f_0 = 0$ the system is normal, thus $f_0 \leq 1$ always. Considering the minimization of free energy density with respect to $\mathscr{A}$ and Ψ it is easy to arrive at equations for the dimensionless functions $\mathscr{H}$ and f_0. The microscopic field is

$$\mathscr{H}(x,y) = \kappa\left[1 + \frac{H - H_{c_2}}{H_{c_2}}\right] - \frac{g(x,y)}{2\kappa}, \qquad (2)$$

with $\boldsymbol{H}$ parallel to the $\boldsymbol{z}$ direction, and the equation for f_0 can be written as

$$\nabla^2(\log g) + 2\kappa^2 = 0, \qquad (3)$$

[1)] The term "first order phase transition" appears in quotes since the sample size is finite.

where $g = f_0^2$ is a positive-definite function. Notice that $\mathscr{H} = \kappa$ for $H = H_{c_2}$ and $f_0 = 0$ ($g = 0$). The most general solution of Eq. (3) has the form[23]

$$g(x,y) = \exp\left[-\kappa^2(x^2+y^2)/2\right]\exp\left[\gamma(x,y)\right], \tag{4}$$

where $\gamma(x,y)$ satisfies Laplace's equation $\nabla^2\gamma(x,y) = 0$. This means that $\gamma(x,y)$ is a harmonic function excluding the locations of vortices, and can be expressed as the real part of an analytic function of $z = x + \mathrm{i}y$. This observation has very important consequences for the microscopic field profile $\mathscr{H}(x,y)$ of Eq. (2), which depends strongly on the structure of $g(x,y)$.

The Gibbs free energy density is given by[4]

$$G_s(H,T) = G_n(H,T) - \frac{1}{8\pi}\frac{(H_{c_2}-H)^2}{(2\kappa^2-1)\beta}, \tag{5}$$

where the parameter $\beta = \langle g^2\rangle/\langle g\rangle^2$ is a geometrical factor independent of κ. The notation $\langle\cdots\rangle$ indicates average over volume. It is important to notice that $\beta \geq 1$ no matter what is the form of $g(x,y)$ because of the Schwartz inequality. In addition, notice that the Gibbs free energy above is a minimum, whenever β reaches its minimum value.

For the purpose of calculating the parameter β and the free energies corresponding to different vortex configurations, the analytical structure of $g(x,y)$ in the complex plane is used to rewrite it as

$$g(z,\bar{z}) = \exp(-\kappa^2 z\bar{z}/2)|P(z)|, \tag{6}$$

where $P(z) = \mathscr{N}\prod_{i=1}^{M}(z-z_i)$. Here, each z_i corresponds to a zero of g in the complex plane, and M is the number of zeros. From now on it is assumed that there is only one vortex with flux Φ_0 at each position z_i, i.e., each zero is non-degenerate. In this case, M corresponds to the number of vortices, and thus the total flux threading the sample is $\Phi = M\Phi_0$. The normalization coefficient $\mathscr{N}$ just guarantees that $g(z,\bar{z}) \leq 1$. Depending on the locations of the zeros of $g(z,\bar{z})$, it is possible to study several possibilities of periodic and quasi-periodic vortex arrangements.

In this study vortex crystals corresponding to triangular and square lattices and vortex quasi-crystals corresponding to the 5-fold Penrose tiling of the plane are considered. Both the square and triangular lattices can be generated via the tiling method, i.e., via the periodic arrangements of identical square tiles or identical lozenges of internal angles (60° and 120°). The Penrose lattice, however, requires quasi-periodic arrangements of two types of tiles (lozenges), one with internal angles 36° and 144° and the other with internal angles 72° and 108°, as shown in Fig. 1.

Without the need of a calculation, it is quite easy to argue why the triangular lattice has the lowest free energy of all periodic lattices for a given magnetic flux density. Simply put the triangular lattice is the most symmetric and the most close-packed. Recall that a vortex in the square lattice has four nearest neighbors at distance a_4 and that a vortex in the triangular lattice has six nearest neighbors at distance a_3. Thus, fixing the flux density per unit cell to be the same for both lattices requires that $HA_3 = \Phi_0$ and $HA_4 = \Phi_0$, where H is the magnetic field, $\Phi_0 = hc/2e$ is the quantum of flux, and $A_3 = a_3^2\sqrt{3}/2$ and $A_4 = a_4^2$ are the area of a unit cell for the triangular and square lattices, respectively. This analysis leads to a unit cell side $a_3 = 1.075(\Phi_0/H)^{1/2}$ for the triangular lattice, and to $a_4 = (\Phi_0/H)^{1/2}$ for the square lattice. This simple exercise shows that for a given flux density $a_3 > a_4$, as is expected since the mutual repulsion of vortices favor the greatest separation of nearest neighbors. A direct computation of the free energy using Eq. (6) supports this analysis giving $\beta_3 = 1.16$ versus $\beta_4 = 1.18$, and shows that the triangular lattice indeed has a lower free energy. Furthermore, a calculation of the free energy for all possible periodic lattices with one vortex per unit cell can be performed since periodic lattices can be parameterized by a single parameter, i.e., the angle between the two generating vectors of two-dimensional lattices. The results of such calculation indeed show that the triangular lattice has the lowest free energy of all periodic vortex lattices in a clean and infinite superconductor.[23]

In an infinite superconductor the quasi-crystalline (5-fold) vortex lattice is unstable because the intervortex distances for the vortices in thin and thick lozenges are different and lead to an increase of the elastic energy. However, the free energy of such configuration has $\beta_5 = 1.22$, which corresponds to a small percentual difference from the triangular lattice. In considering all the possible quasi-periodic tilings of the infinite plane which are compatible with 5-fold symmetry, the Penrose tiling is the most close-packed, just like the triangular lattice is the most close packed periodic structure of the infinite plane. A beautiful proof using C-cluster theory and cluster energies (based on pairwise interactions) is described in the literature,[24,25] which shows that the Penrose tiling is the unique ground state of a quasi-crystal. This result can be translated into the vortex language, by simply considering vortices as point particles arranged in C-clusters, and use the results from the literature[24,25] to infer that the Penrose tiling has the most close-packed structure for quasi-periodic vortex arrangements. Thus, for a given magnetic flux density the 5-fold Penrose vortex tiling has the lowest energy of all vortex tilings compatible with 5-fold symmetry.

This conclusion can also be tested by numerical calculation of a given vortex lattice configuration. For example, the five-fold arrangement consisting of concentric pentagonal shapes (with free energy gain ΔG_{5p} and β_{5p}) shown in Fig. (2a) and extended to the entire two dimensional plane has higher free energy than the corresponding Penrose lattice (with free energy gain ΔG_5 and β_5) shown in Fig. (2b). The ratio of free

energy gains is $\Delta G_5/\Delta G_{5p} = \beta_{5p}/\beta_5 \approx 1.03$. However, the beauty of the arguments above is that one does not need to compute the free energy of an infinite number of vortex configurations in order to decide on the most likely candidate for a given class of constraints in an infinite superconductor. If the constraint is quasi-periodicity with 5-fold symmetry then the Penrose lattice always wins. If the constraint is periodicity or quasi-periodicity, then the triangular lattice always wins. All these 5-fold vortex tilings (including Penrose) are clearly unstable with respect to the triangular array in a clean and infinite superconductor (plane), however in confined geometries the situation may be different. Thus the key question is, can the Penrose vortex lattice have lower energy than a triangular vortex lattice?

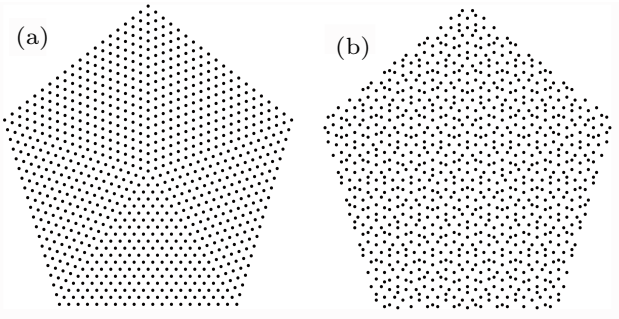


Fig. 2. Five-fold symmetric vortex arrangements corresponding to (a) concentric pentagonal shapes and (b) the Penrose lattice arrangements.

As mentioned above, the values of β for the triangular, and Penrose tiling are respectively $\beta_3 = 1.16$, and $\beta_5 = 1.22$, as obtained using the representation in Eq. (6). This immediately indicates that the triangular lattice has lower free energy than the 5-fold vortex quasi-crystal (Penrose tiling), as discussed. However, since the free energy difference between the triangular and 5-fold vortex quasi-crystal is only a few percent, the use of samples with appropriate shapes and boundaries can favor 5-fold symmetry as the sample size gets smaller. Given that the close-packed 5-fold Penrose vortex tiling has the lowest free energy of all 5-fold symmetric vortex tilings of a clean and infinite superconductor for a given flux density, we can envision the stabilization of this structure by imposing boundary conditions consistent with its symmetry. This can be achieved in the pentagonal geometry suggested here. Thus, we discuss next the boundary effects and the magnetic field versus temperature phase diagram.

3. Boundary effects and phase diagram

In order to investigate how boundary effects can modify the total free energy of the system, a sample in the shape of a pentagon cylinder of side ℓ and height L is considered. Imposing that no currents flow through the sample boundaries leads to the condition

$$\hat{\boldsymbol{n}} \cdot [-\mathrm{i}\boldsymbol{\nabla} - 2\pi \boldsymbol{A}/\Phi_0]\,\Psi(x,y) = 0 \tag{7}$$

at all five side faces. The unit vector $\hat{\boldsymbol{n}}$ points along the normal direction of each facet of the pentagon cylinder. The boundary conditions can be translated in terms of the harmonic function $\gamma(x,y)$ as

$$n_x \frac{\partial \gamma}{\partial y} - n_y \frac{\partial \gamma}{\partial x} = \kappa(n_x y - n_y x), \tag{8}$$

where n_x and n_y are the x and y components of the normal unit vector $\hat{\boldsymbol{n}}$ at each one of the pentagon cylinder side faces. The solution for this boundary value problem can be obtained using a Schwarz–Christoffel conformal map of the pentagon into a semi-infinite plane

$$\frac{\mathrm{d}z}{\mathrm{d}w} = C(w - x_1)^{-2/5}(w^2 - x_2^2)^{-2/5}(w^2 - x_3^2)^{-2/5}, \tag{9}$$

where the vertices of the pentagon located at z_i are mapped into the points $(x_1, \pm x_2, \pm x_3)$ on the real axis of the w-plane. The full solution of this problem is complicated, and requires heavy use of numerical methods.[26] However, the free energy density can be estimated when the bulk solution in Eq. (6) is treated as a variational solution of the boundary value problem determined by Eqs. (3), (8), and (9).

The Gibbs free energy density difference $\Delta G = G_3 - G_5$ between the triangular and the 5-fold quasi-periodic Penrose structure then becomes

$$\Delta G = -\frac{1}{8\pi}\frac{(H_{c_2} - H)^2}{(2\kappa^2 - 1)\beta^*} + \frac{H_c^2}{4\pi}\varepsilon(H), \tag{10}$$

where $\beta^* = \beta_3\beta_5/(\beta_5 - \beta_3)$, H_c is the thermodynamic critical field, and $\varepsilon = (\alpha_3 - \alpha_5)(2R_e + \alpha_3 + \alpha_5)/2R_e^2$, with $\alpha_3 = 0.93a_0$, $\alpha_5 = 0.90a_0$, and $a_0 = \sqrt{\Phi_0/H}$. The effective length of the sample $R_e = \ell/\sqrt{4 - \tau^2}$, where $\tau = 2\cos(\pi/5)$ is the golden mean. Here, R_e corresponds to the radius of the circle that circumscribes the pentagonal sample.

This expression for ΔG is valid only when $H \gg \Phi_0/R_e^2$. The second term in ΔG takes into account the boundary mismatch energy, and indicates that as the size of the pentagon cylinder gets smaller it becomes more favorable to have a 5-fold quasi-crystal rather than a regular triangular lattice. Notice, however, that when $R_e \to \infty$ the triangular lattice has lower Gibbs free energy as it must, and no transition to a 5-fold quasi-crystal occurs. Thus, this possible transition may occur for finite sized samples only. From the condition that $\Delta G = 0$ we obtain

$$H_Q(T) = H_{c_2}(T)\left[1 - \kappa^*\sqrt{\beta^*\varepsilon(H_Q)}\right], \tag{11}$$

where the transition to a quasi-crystal occurs. Here, $\kappa^* = \sqrt{2\kappa^2 - 1}/\kappa$.

The phase diagram for a superconductor with $\kappa = 20$, $H_{c_2}(0) = 10$ T and $R_e = 10^{-6}$ m is shown in Fig. 3 using $H_{c_2}(T) = H_{c_2}(0)\left[1 - (T/T_c)^2\right]$ (It is noted that the critical field $H_{c_3}(T)$ for surface superconductivity is not shown in Fig. 3.). Recall that the flux quantum $\Phi_0 = hc/2e = 2.07 \times$

10^{-15} T·m^2, and that the area of the pentagonal sample is $A = (5/2)R_e^2 \cos(2\pi/5)$. Notice that the number of vortices M_Q close to H_Q can be quite large at low temperatures. For the parameters above $M_Q = H_Q(0)A/\Phi_0 \approx 4000$, and the vortex quasi-crystal structure can be extracted, as shown in Fig. 2.

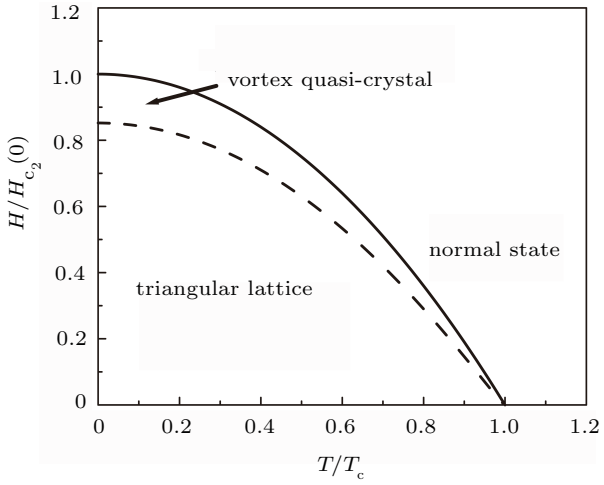


Fig. 3. H–T phase diagram for a pentagonal cylinder cut out of a regular cylinder of radius for $R_e = 10^{-6}$ m. The solid and dashed lines represent H_{c_2} and H_Q, respectively, while H_{c_1} is not shown. The superconductor is assumed to have $\kappa = 20$, $H_{c_2}(0) = 10$ T.

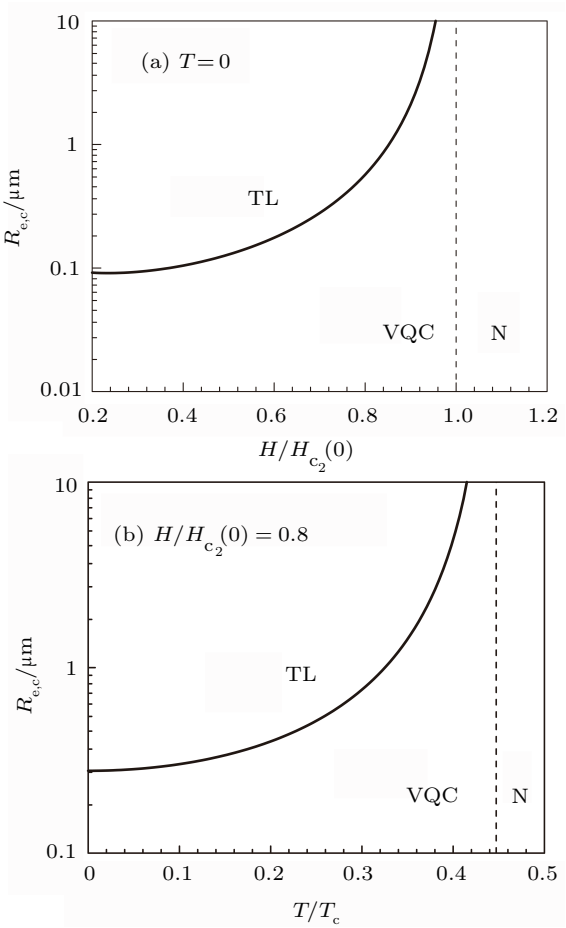


Fig. 4. Critical value of superconducting sample size $R_{e,c}$ in logarithmic scale as a function of (a) H for a given $T < T_c$, and as a function of (b) T for a given $H < H_{c_2}(0)$. Parameters used in these plots are the same as in Fig. 3 and the regions labeled TL, VQC, and N correspond to triangular lattice, vortex quasi-crystal, and normal phases, respectively.

However, the phase diagram becomes less precise at lower magnetic fields, since the low value of H reduces substantially the number of vortices, and the condition $H \gg \Phi_0/R_e^2$ is violated. Furthermore, for fixed $H_{c_2}(0)$, one can find the critical value of $R_{e,c}$ below which the vortex quasi-crystal phase appears. Curves of $R_{e,c}$ versus T or H can be obtained and are shown in Fig. 4. Notice that the critical $R_{e,c}$ increases with increasing H (T) for a fixed T (H). Notice also that for a fixed sample size, and fixed magnetic field the vortex-quasi crystal phase always occurs at higher temperatures due to its higher entropy.

In order to address the signature of the crystal-quasi-crystal phase transition, we discuss next the thermodynamic properties including magnetization and entropy of the triangular and Penrose lattices in the pentagonal geometry.

4. Thermodynamics: changes in magnetization and entropy

The jump of the magnetization $\Delta M (= M_3 - M_5)$ as a function of temperature at the critical field H_Q can be calculated from the Gibbs free energy, leading to

$$\Delta M = \frac{H_{c_2}}{4\pi}\left[-\frac{\gamma^*}{(2\kappa^2-1)\beta^*} + \Delta M_s\right], \tag{12}$$

where $\gamma^* = \kappa^*\sqrt{\beta^*\varepsilon}$ and $\Delta M_s = (\alpha_3 - \alpha_5)(R_e + \alpha_3 + \alpha_5)/4\kappa^2 R_e^2(1-\gamma^*)$. A plot of ΔM is illustrated in Fig. 5 for the same parameters in Fig. 3. Using these parameters produces jump discontinuities $\Delta M \approx -0.060$ Gs (1 Gs $= 10^{-4}$ T) at $T = 0$, and $\Delta M \approx -0.028$ Gs at $T = 0.8T_c$. Although a measurement of magnetic field in the order of mGs is plausible in experiments, one may also consider preparing an array of identical pentagonal cylinders to enhance the overall value. Notice that $\Delta M < 0$ indicates that the 5-fold vortex quasi-crystal is denser than the triangular vortex lattice at H_Q, being at best a few percent denser at $T = 0$.

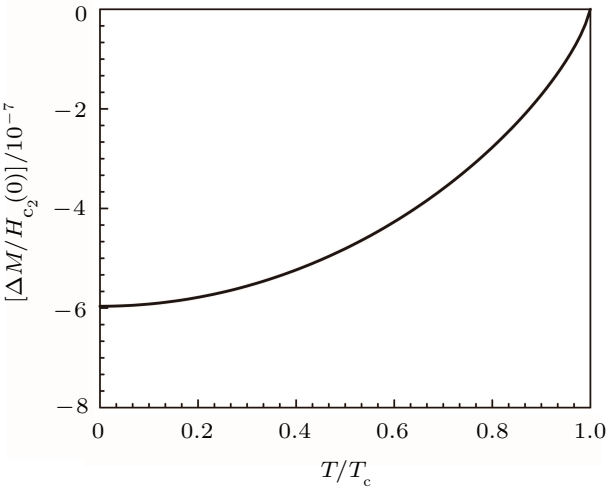


Fig. 5. The jump discontinuity $\Delta M = M_3 - M_5$ at the critical field H_Q for various reduced temperatures T/T_c, using the same parameters of Fig. 3.

In addition to magnetization measurements, it is also interesting to perform calorimetric experiments. However, specific heat measurements are very difficult because they require large samples. Since sample size is important for the present discussion it is not clear that such experiments can be successfully performed. Nevertheless, the thermodynamic relationship between the magnetization and entropy jumps is revealed in the Clapeyron equation

$$\Delta S = S_3 - S_5 = -\Delta M \, \mathrm{d}H_{\mathrm{Q}}/\mathrm{d}T. \tag{13}$$

Since $\mathrm{d}H_{\mathrm{Q}}/\mathrm{d}T < 0$, and $\Delta M < 0$ implies that $\Delta S < 0$, the entropy S_3 of the triangular vortex lattice is less than the entropy S_5 of the 5-fold vortex quasi-crystal, indicating that latent heat $L = T\Delta S$ is required to cause this phase transition.

Thermodynamic quantities can provide a good understanding of properties averaged over the entire sample, and can characterize the signature of the crystal-quasi-crystal phase transition. However, as discussed above, a good measurement of these quantities may require an array of identical samples, which introduces experimental complexity and difficulty. As another possibility, the use of local probes discussed next is much desired in order to reveal the change in structure from a triangular vortex crystal to a 5-fold vortex quasi-crystal. For instance, neutron scattering, Bitter decoration or scanning tunneling microscopy (STM) experiments may help elucidate the structure of the vortex arrangement in mesoscopic samples.[27]

5. Local Probes: neutron diffraction and scanning tunneling microscopy

In neutron diffraction experiments periodic or quasi-periodic variations of $\mathscr{H}(x,y)$ will result in Bragg peaks. The position of these peaks determine the characteristic length scale of the vortex structure and its symmetry. The neutron scattering amplitude in the Born approximation is

$$b(\boldsymbol{q}) = \frac{M_{\mathrm{n}}}{2\pi\hbar^2} \int \mu_{\mathrm{n}} H(\boldsymbol{r}) \exp(\mathrm{i}\boldsymbol{q}\cdot\boldsymbol{r}) \, \mathrm{d}\boldsymbol{r}, \tag{14}$$

where $\mu_{\mathrm{n}} = 1.91 e\hbar/M_{\mathrm{n}}c$ is the neutron magnetic moment and the M_{n} is the neutron mass. The scattering amplitude $b(\boldsymbol{q})$ is directly proportional to the Fourier transform $H(\boldsymbol{q})$ [$\mathscr{H}(q_x,q_y)$] of the microscopic field $H(\boldsymbol{r})$ [$\mathscr{H}(x,y)$] of Eq. (2). The neutron scattering cross section

$$\sigma(q_x,q_y) = 4\pi^2 |b(q_x,q_y)|^2 \tag{15}$$

has sharp peaks at $(q_x,q_y) = (0,0)$ (central peak) and at $(q_x,q_y) = (\pm q_{xNm}, \pm q_{yNm})$ (first Bragg peaks), where $q_{xNm} = Q_N \cos(m\pi/N)$ and $q_{yNm} = Q_N \sin(m\pi/N)$, with $m = 0,1,\ldots,N-1$. For the triangular lattice $N = 3$ the first Bragg peak occurs at $|Q_3| = 2.31 \times \pi/d_3$, where d_3 is the lattice spacing. For the 5-fold vortex quasi-crystal (Penrose lattice, $N = 5$) the first Bragg peak occurs at $|Q_5| = 2.46 \times \pi/d_5$, where d_5 is the side of a tile. Since the sample size is important for the observation of a 5-fold quasi-crystal, neutron scattering experiments may be difficult to perform.

However, Bitter decoration might be a useful technique if magnetic nano-particles could be used to decorate the magnetic field profile, and then be seen by a scanning tunneling microscope (magnetic or non-magnetic). Furthermore, it may be possible to use just an STM to scan over the pentagonal sample and probe the local density of states which is substantially different inside and outside of vortex cores, due to the presence of vortex cores states. In this case, it may also be useful to make a periodic pattern of pentagonal samples, and obtain an ensemble average. It should be possible as well to perform STM scans at different fields and temperatures in the vicinity of $H_Q(T)$, which would reveal the real space locations of vortices. The pattern obtained could then be Fourier transformed (FT) to obtain a 6-fold pattern for the triangular vortex lattice and a 10-fold pattern for the 5-fold vortex quasi-crystal, which is shown in Fig. 6.

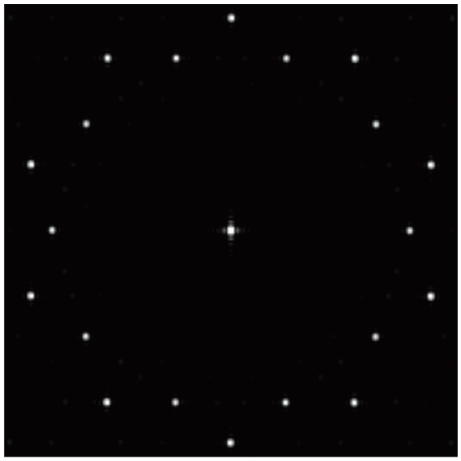


Fig. 6. First peaks of the square of the Fourier transformed (FT) pattern for the 5-fold vortex quasi-crystal (Penrose lattice). Notice that the pattern is 10-fold symmetric, unlike the case of the triangular vortex lattice, where the pattern is 6-fold symmetric.

Now that the phase diagram, thermodynamics, and the local signatures of a vortex quasi-crystal have been discussed, it is important to say a word on the stability of such structures. Even if one were to object that the 5-fold Penrose vortex tiling is not the ground state of a vortex quasi-crystal (at high magnetic fields and low temperatures) compatible with the 5-fold symmetry of a perfect pentagonal sample, a stability analysis shows that the Penrose vortex tiling is stable in this geometry, which is a sufficient condition for its observability. A stability analysis in the free energy can be performed by moving the vortices away from their equilibrium positions z_i to $z_i + \delta z_i$. The eigenvalues associated with these displacements indicate that for $H > H_{\mathrm{Q}}(T)$ the vortex quasi-crystal lattice is stable at low temperatures for small displacements, and therefore is potentially realizable in mesoscopic samples.

6. Final comments and conclusions

Before concluding, we would like to make several comments in connection with the approximations used and the observability of the vortex quasi-crystal phase discussed.

First, it should be emphasized that our free energy analysis provides a preliminary understanding of the vortex quasi-crystal phase, but further detailed numerical work is necessary. For instance, the vortex quasi-crystal sitting on a Penrose lattice is only one possible state in a pentagonal superconducting sample at high magnetic fields (large number of vortices). Although we have shown that this state has lower free energy than a triangular lattice in the high field regime (large number of vortices) and low temperatures, and that it is the ground state for a perfect pentagonal sample at high fields and low temperatures, we cannot rule out other possibilities based on the present calculation such as the appearance of a liquid state at higher temperatures, where the triangular vortex lattice melts as a whole or the vortex quasi-crystal melts as a whole, before or after a vortex quasi-crystal sets in. This additional situation is possible due to the two-dimensionality of our geometry, which allows for the appearance of dislocation-mediated melting. In infinite two-dimensional samples, it is well known that melting of triangular lattices is possible via the Kosterlitz–Thouless–Halperin–Nelson–Young (KTHNY) mechanism,[28–31] where dislocations proliferate throughout the sample producing a hexatic liquid crystal at finite temperatures. These processes also occur on finite "two-dimensional" samples of all types (circular, triangular, square), as well as the pentagonal sample described here, and need careful consideration. A hexatic vortex liquid phase may be possible at high fields and finite temperatures for a disk since the C_∞ group of the disk contains the C_6 group of six-fold rotations. However, for a pentagonal sample, the six-fold symmetry of the hexatic phase is not compatible with the five-fold symmetry of the pentagon and the C_5 group of five-fold rotations of the pentagon does not include the C_6 group of six-fold rotations. Therefore, for a pentagonal geometry, even if a hexatic vortex liquid phase appears due to the KTHNY mechanism at some intermediate magnetic field, it cannot be the ultimate phase for a pentagonal sample in the high-magnetic-field/low-temperature regime, where the sample boundaries play an essential role.

Second, there is no full compatibility of the 5-fold Penrose lattice with a pentagon cylinder geometry containing surface imperfections. The presence of surface imperfections (a nearly inevitable experimental difficulty) breaks the perfect 5-fold symmetry, and the appearance of disclinations and dislocations at the edges of the sample is possible at high magnetic fields even at zero temperature. As a result there is an additional possibility of a solid (crystal or quasi-crystal) vortex structure in the center of the sample, which melts or gets disordered at the sample boundaries, because of the resulting symmetry incompatibility introduced by surface imperfections. In our calculations, we have assumed a perfect pentagonal geometry, but the effects of surface imperfections on the vortex arrangement need to be taken into account in a more realistic calculation, since they break the perfect C_5 symmetry of the boundaries and make them incompatible to the perfect C_5 symmetry of the Penrose lattice. The same kind of symmetry incompatibilities introduced by surface imperfections are also found in hexagonal samples, where the triangular vortex lattice should melt or get disordered at the sample boundaries. For instance, a perfect hexagonal sample favors a perfect triangular lattice at high fields and low temperatures, because of the perfect compatibility between the lattice and the boundaries. However, imperfections break the perfect C_6 symmetry of the hexagonal boundaries and make them incompatible to the perfect C_6 symmetry of the triangular lattice, thus leading to a melted/disordered triangular lattice at the sample edges. For instance, these kinds of symmetry incompatibilities between the vortex lattice and the sample boundaries have already been studied in mesoscopic disks,[32] where at high magnetic fields (large number of vortices) the triangular vortex lattice is found at the center, but is melted/disordered at the edge, because the disk's circular boundary (C_∞) does not have perfect 6-fold symmetry (C_6), and thus allows for the appearance of disclinations and dislocations. Therefore, in general, we expect to have melting/disordering of the vortex lattice in all cases where there is an incompatibility between the natural symmetry of the vortex lattice at high magnetic fields and the symmetry of the boundaries of the sample.

Third, the number of vortices in superconducting samples is restricted by $N_{\max} = H_{c_2}(0)A/\Phi_0$, which means that for superconductors with high H_{c_2} a large number of vortices is possible. One can make a simple estimate for $N_{\max}$ by using the Ginzburg-Landau relation $H_{c_2} = \Phi_0/(2\pi\xi^2)$, leading to $N_{\max} \sim [R_e/\xi(T=0)]^2$. For conventional type II superconductors, the number $N_{\max}$ is only about $10^1 \sim 10^2$, thus the thermodynamic limit and hence the definition of the quasi-crystal phase is questionable. However, for materials with short coherence length (and large upper critical fields), such as high-T_c superconductors, where $\xi(T=0)$ is about $10^1 \sim 10^2$ Å, then $N_{\max}$ can be as large as $10^4 \sim 10^5$, and the quasi-crystalline structure can be well defined and observed. Thus, the observation of a vortex quasi-crystal state is more likely to occur in short coherence length superconductors at low temperatures and high magnetic fields.

Finally, strong disorder in the center and throughout the sample can also destroy the quasi-crystal structure due to the pinning of vortices, however, clean mesoscopic superconducting materials nearly disorder free already exist and shell struc-

tures have been observed for Niobium samples of μm sizes.[33] Thus, we suspect that experimentally this should not be an issue as vortex lattices (triangular) are routinely observed in reasonably clean superconducting samples. Therefore, the choice of pentagonal mesoscopic samples of superconductors with sufficiently large H_{c_2} should allow for the observation of the vortex quasi-crystal state.

In summary, we have shown that vortex quasi-crystals may be experimentally observed in mesoscopic samples of type II superconductors with large upper critical fields (short coherence lengths). By taking into account boundary effects, sample shape and size, we proposed that a first order phase transition occurs between a vortex crystal and a vortex quasi-crystal, as magnetic field and temperature are varied.

Acknowledgment

We would like to thank Wai Kwok and Franco Nori for references, the Aspen Center for Physics for their hospitality, and support from a grant from the Simons Foundation.

References

[1] Crabtree G W and Nelson D R 1997 *Physics Today*, pp. 38–45
[2] Safar H, Gammel P L, Huse D A, Bishop D J, Lee W C, Giapintzakis J and Ginsberg D M 1993 *Phys. Rev. Lett.* **70** 3800
[3] Kwok W K, Fendric J, Fleshler S, Welp U, Downey J and Crabtree G W 1994 *Phys. Rev. Lett.* **72** 1092
[4] Abrikosov A A 1957 *Sov. Phys. JETP* **5** 1174
[5] Koch R H, Foglietti V, Gallagher W J, Koren G, Gupta A and Fisher M P A 1989 *Phys. Rev. Lett.* **63** 1511
[6] Shechtman D, Blech I, Gratias D and Cahn J W 1984 *Phys. Rev. Lett.* **53** 1951
[7] Sá de Melo C A R 2007 "Vortex Quasi-crystals", manuscript No. LH7266, 05Aug99. See this unpublished work in preprint No. cond-mat/0703156
[8] Misko V, Savel'ev S and Nori F 2005 *Phys. Rev. Lett.* **95** 177007
[9] Misko V, Savel'ev S and Nori F 2006 *Phys. Rev. B* **74** 024522
[10] Villegas J E, Montero M I, Li C P and Schuller I K 2006 *Phys. Rev. Lett.* **97** 027002
[11] Kemmler M, Gürlich C, Sterck A, Pöhler H, Neuhaus M, Siegel M, Kleiner R and Koelle D 2006 *Phys. Rev. Lett.* **97** 147003
[12] Silhanek A V, Gillijns W, Moshchalkov V V, Zhu B Y, Moonens J and Leunissen L H A 2006 *Appl. Phys. Lett.* **89** 152507
[13] Denton A R and Lowen H 1998 *Phys. Rev. Lett.* **81** 469
[14] Matthews M R, Anderson B P, Haljan P C, Hall D S, Wieman C E and Cornell E A 1999 *Phys. Rev. Lett.* **83** 2498
[15] Zwierlein M W, Abo-Shaeer J R, Schirotzek A, Schunck C H and Ketterle W 2005 *Nature* **435** 1047
[16] Tung S, Schweikhard V and Cornell E A 2006 *Phys. Rev. Lett.* **97** 240402
[17] Geim A K, Griogorieva I V, Dubonos S V, Lok J G S, Maan J C, Filippov A E and Peeters F M 1997 *Nature* **390** 259
[18] Geim A K, Dubonos S V, Palacios J J, Grigorieva I V, Henini M and Schermer J J 2000 *Phys. Rev. Lett.* **85** 1528
[19] Chibotaru L F, Ceulemans A, Bruyndoncx V and Moshchalkov V V 2000 *Nature* **408** 833
[20] Chibotaru L F, Ceulemans A, Bruyndoncx V and Moshchalkov V V 2001 *Phys. Rev. Lett.* **86** 1323
[21] Dikin D A, Chandrasekhar V, Misko V R, Fomin V M and Devreese J T 2003 *Eur. Phys. J. B* **34** 231
[22] Berdiyorov G R, Milosevic M V and Peeters F M 2006 *Phys. Rev. Lett.* **96** 207001
[23] Saint-James D, Sarma G and Thomas E J 1969 *Type II superconductivity* (Oxford: Pergamon Press) Chap. 3
[24] Steinhardt P J and Jeong H C 1996 *Nature* **382** 431
[25] Jeong H C and Steinhardt P J 1997 *Phys. Rev. B* **55** 3520
[26] Henrici P 1986 *Applied and computational complex analysis* (New York: John Wiley and Sons) Vol. III, Chap. 16
[27] Sun L, Huo Y, Zhou C, Liang J H, Zhang X Z, Xu Z J, Wang Y and Wu Y Z 2015 *Acta Phys. Sin.* **64** 197502 (in Chinese)
[28] Kosterlitz J M and Thouless D J 1973 *J. Phys. C* **6** 1181
[29] Halperin B I and Nelson D R 1978 *Phys. Rev. Lett.* **41** 121
[30] Halperin B I and Nelson D R 1979 *Phys. Rev. B* **19** 2457
[31] Young A P 1979 *Phys. Rev. B* **19** 1855
[32] Cabral L R E, Baelus B J and Peeters F M 2004 *Phys. Rev. B* **70** 144523
[33] Grigorieva I V, Escoffier W, Richardson J, Vinnikov L Y, Dubonos S and Oboznov V 2006 *Phys. Rev. Lett.* **96** 077005